applied sciences

MDPI

Article

The Spatial Distribution Characteristics and Possible Influencing Factors of Landslide Disasters in the Zhaotong Area, Yunnan Province of China

Wantong Wang [1,2,3], Siyuan Ma [2,3], Wujian Yan [1] and Renmao Yuan [2,3,*]

[1] Lanzhou Institute of Seismology, China Earthquake Administration, Lanzhou 730000, China; wwt@ies.ac.cn (W.W.); yanwj1980@126.com (W.Y.)
[2] Institute of Geology, China Earthquake Administration, Beijing 100029, China; masiyuan@ies.ac.cn
[3] Key Laboratory of Seismic and Volcanic Hazards, Institute of Geology, China Earthquake Administration, Beijing 100029, China
* Correspondence: yuanrenmao@ies.ac.cn

Abstract: The Zhaotong area in Yunnan Province stands out as one of the most susceptible areas to landslide disasters. The landslide susceptibility of the Zhaotong area can be attributed to its steep terrain, fractured rock formations and strong rainfall, compounded by its frequent seismic activity. This study utilized landslide data provided by the Zhaotong City Natural Resources and Planning Bureau and visually interpreted from high-resolution satellite images of Google Earth to establish the landslide database of the Zhaotong area, including 161 landslides and 3646 potential geological disasters. The distribution characteristics and possible influencing factors of landslides within the Zhaotong area were analyzed using the aforementioned data. The results show that the spatial distribution of landslides and potential geological disasters is roughly consistent; the most concentrated landslides occurred at the junction of Yiliang County, Zhaotong City, and Daguan County, indicating the necessity to enhance surveillance of these landslide-prone areas. The relationship of landslide locations and different influencing factors suggests that elevation, slope angle, and distance to rivers are closely related to landslide occurrence. Landslides are more likely to occur in areas with lower elevations with slope angles ranging from 10° to 40° and near river channels.

Keywords: Zhaotong area; landslide disasters; influencing factors; distribution pattern; Google Earth; statistical analysis

Citation: Wang, W.; Ma, S.; Yan, W.; Yuan, R. The Spatial Distribution Characteristics and Possible Influencing Factors of Landslide Disasters in the Zhaotong Area, Yunnan Province of China. *Appl. Sci.* **2024**, *14*, 5093. https://doi.org/10.3390/app14125093

Academic Editor: Syed Minhaj Saleem Kazmi

Received: 21 May 2024
Revised: 6 June 2024
Accepted: 7 June 2024
Published: 12 June 2024

1. Introduction

The Zhaotong area in Yunnan Province is identified as one of the areas that are severely threatened by earthquakes and rainfall. This region is characterized by steep topography, fragmented rocks, and abundant rainfall compounded by active faults, which caused frequent occurrences of landslides and debris flows. For example, in 1991, a colossal landslide struck Touzhai Gou Village, located in Panhe Township, Zhaotong City. The landslide was estimated to have a volume of 20 million m^3, plummeting vertically over a distance of 760 m [1]. This event led to the tragic loss of 216 lives, with seven injuries reported. Additionally, 202 houses were destroyed, and the direct economic losses were estimated at approximately RMB 12 million. The 1917 Ms 6.7 Daguan Jilipu earthquake triggered massive collapses and landslides in the Daguan River canyon area, burying over 500 military personnel [2]. The 2014 Ludian earthquake resulted in 10,560 landslides [3], with the most significant occurrence recorded at the Hongshiyan and Ganjiazhai area. Notably, the Hongshiyan landslide with a volume of 10 million m^3 obstructed the Niulan River and formed a barrier lake with a volumetric capacity of 260 million m^3. During the 13 July 2010, the Xiaohe Village in Qiaojia County experienced a catastrophic flood and mudslide, leading to the tragic loss of 19 lives, with 26 individuals reported missing

and 43 sustaining injuries. These large-scale landslides and debris flows not only caused significant casualties and severe damage to the local economy but also irreversibly altered the local landscape. Therefore, the susceptibility assessment of potential landslides in seismically active regions is crucial to effectively reduce the impact of such disasters.

The analysis of the development characteristics and spatial distribution of landslides in the Zhaotong area is important for assessing the potential landslide susceptibility in the area. Various controlling factors influence the occurrence of landslides, including the geological setting, slope structure type, and topographical conditions, as well as earthquakes and rainfall [4–6]. Among these controlling factors, rainfall and earthquakes are the most significant. Zou, Qi et al. (2022) [7] employed Geographic Information System (GIS) technology to explore the spatial distribution of coseismic landslides triggered by the 2014 Ludian earthquake, and the results showed that slope gradient and proximity to the seismogenic fault are critical factors in determining the spatial distribution of seismic landslides. Furthermore, it was observed that landslide number density exponentially decreases with an increasing distance from the seismogenic fault and follows a Weibull cumulative distribution with increasing slope gradient. Chen, Liu et al. (2018) [8] applied the Newmark method to calculate the minimum critical accelerations for the slope failures of the Ludian event. Their findings indicated that the spatial distribution of coseismic landslides in most regions was influenced by geological factors, whereas a minority of areas were affected by a combination of geological, topographical, and complex seismic source structures. He, Xu et al. (2021) [9] analyzed the spatial distribution characteristics of landslides of the Mw 5.1 Qiaojia earthquake using the landslide abundance index. Their analysis showed that landslides predominantly aligned in the northwest–southeast direction, paralleling the seismic intensity zones and the strike of the Xiaohe–Baogunao fault (XBF). These results indicated that the seismogenic fault of the Qiaojia earthquake may be a concealed branch of the XBF, likely activated due to the release of accumulated elastic strain from the earlier Ludian earthquake within the same tectonic stress regime. Jin, Cui et al. (2023) [10] used the landslide data of the Mw 5.7 Yiliang earthquake, selecting nine influencing factors to develop a coseismic landslide probability model using Bayesian probability method and logistic regression model. The model was applied to predict landslides for the Ludian earthquake, demonstrating a good fit and confirming the similarity in landslide characteristics between the Yiliang and Ludian earthquakes. Jia, Chen et al. (2016) [11] analyzed the differences between the landslides triggered by the Ludian earthquake and the landslide triggered by the Jinggu earthquake, and the result revealed that these differences mainly resulted from four factors: earthquake intensity, population density, building seismic resistance, and geological environment. Such studies often focused on specific rainfall or seismic events in affected regions, with few studies conducted on the developmental characteristics and spatial distribution patterns of landslide disasters in the Zhaotong area. Moreover, the selection of influencing factors for landslide disasters is greatly influenced by the geological environment, climatic factors, and human engineering activities in the study area, which limits the spatial distribution of landslide disasters and the analysis of influencing factors in this region.

In this study, landslide data provided by the Bureau of Natural Resources and Planning, combined with visual interpretation of high-resolution satellite images from Google Earth platform, were utilized to obtain information on 161 landslides and 3646 potential geological disasters in the Zhaotong area. Six influencing factors were selected for investigation: elevation, slope angle, slope orientation, geological unit, distance to rivers, and rainfall. This study not only analyzes the correlation between landslide occurrences and such potential factors based on statistical data, but also further examines the relationship between landslide occurrences and population distribution. The main objective of this work is to figure out how the potential factors exert influence on the spatial distribution of landslides, which can provide essential data and scientific support for landslide prevention and mitigation planning in the Zhaotong area.

2. Study Area

The Zhaotong area, situated in the northeastern part of Yunnan Province, China, spans geographical coordinates ranging from 26°55′ to 28°36′ N latitude and 102°5′ to 105°19′ E longitude (Figure 1a). It is a prefecture-level city located in the northeast corner of Yunnan Province of China, bordering the provinces of Guizhou to the south and southeast and Sichuan to the northeast, north, and west. The Zhaotong area comprises nine counties with a total area of 23,000 km^2. It is inhabited by 6.33 million people from 24 ethnic groups.

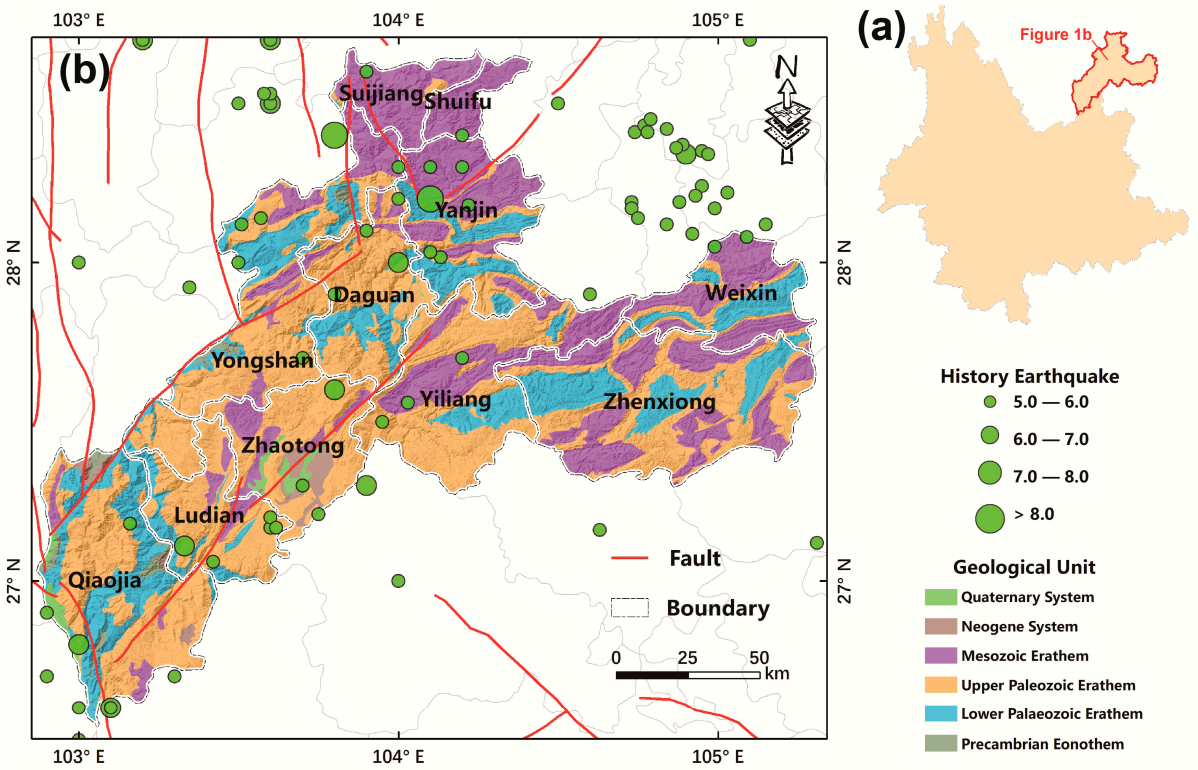

Figure 1. (**a**) Map showing the location of Zhaotong, Yunnan Province; (**b**) the geological unit distribution, earthquakes, and tectonic setting of the Zhaotong area.

The Zhaotong area is situated in the hinterlands of the Wumeng Mountains at the confluence of the Yunnan, Guizhou, and Sichuan Provinces, along the downstream region of the Jinsha River. This location forms a transitional zone where the Sichuan Basin rises to the Yunnan–Guizhou Plateau, characterized by complex geological structures and distinct geomorphological features. The terrain slopes from the southwest to the northeast with an elevation difference of 3773 m, ranging from the highest point at Dayao Mountain in Qiaojia County at 4040 m, to the lowest point at Gunkan Dam in Shuifu County at 267 m, with an average elevation of 1685 m. The annual average precipitation of the study area is between 660 and 1230 mm, concentrated primarily from May to October.

The strata outcropped in the Zhaotong area range from the Sinian to the Quaternary systems (Figure 1b). The most widely distributed are the Paleozoic, dominated by marine sedimentary limestone and mudstone, with the Permian lithology primarily composed of basalt. The Mesozoic shifted to terrestrial deposits with the Triassic strata characterized mainly by limestone, sandstone, and clastic rocks. The Cenozoic are primarily found near the Zhaotong Basin, consisting mostly of loose clay, loam, and gravel. The region has numerous active faults, including the Zhaotong–Ludian fault zone (late Pleistocene), the Lianfeng fault (middle Pleistocene), and the Xiaojiang fault zone (Holocene), among others. This area is prone to frequent seismic activity, with 32 earthquakes of Ms 5.0 between 1844 and 2023. The largest recorded earthquake was a Ms 7.1 earthquake event in 1974 in Daguan, Yunnan.

3. Methods and Data

3.1. Methods

Due to its capability to obtain global high-resolution and ultra-high-resolution three-dimensional satellite images, and its visual interpretation method, the Google Earth platform has been extensively utilized for landslide identification [12–14]. In this study, satellite images from 2012 to 2020 on the Google Earth platform were used to further validate the locations of landslides provided by the Zhaotong City Natural Resources and Planning Bureau. According to the interpretation signs such as topographic features and vegetation cover in the region, clear differences in color and texture in images before and after landslides were observed, which facilitated the identification of landslide boundaries (Figure 2). Field surveys were conducted in Ludian, Qiaojia, Yiliang, and Yanjin counties—areas with concentrated landslide activities—to further validate the accuracy of the interpreted data on landslides and potential landslides in the Zhaotong area. Ultimately, 161 landslides and 3646 potential geological disasters have been determined since 2012 in the Zhaotong area.

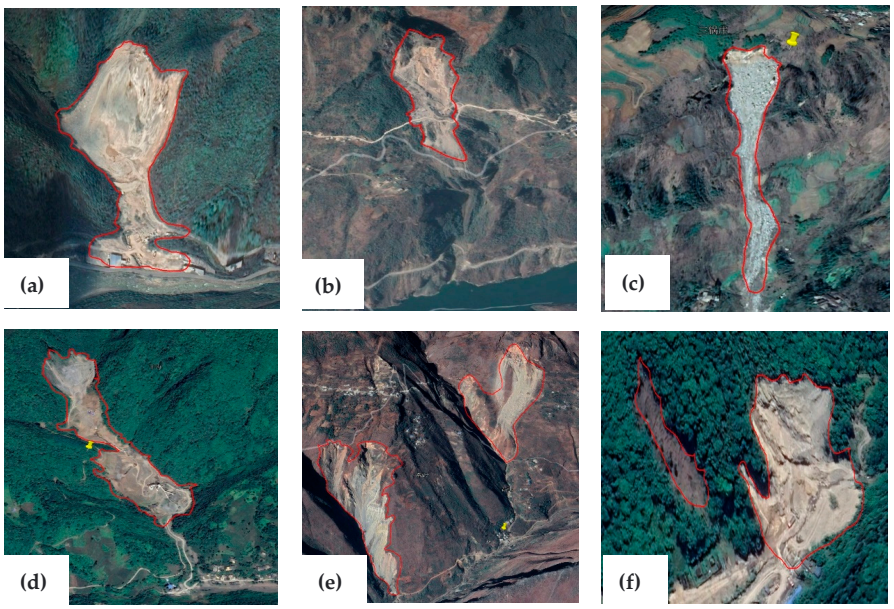

Figure 2. Map showing the satellite images of typical landslide disasters in the Zhaotong area provided by Google Earth: (**a**) The geographical location is 27.50° N, 103.98° E. (**b**) The geographical location is 27.28° N, 103.22° E. (**c**) The geographical location is 27.22° N, 103.25° E. (**d**) The geographical location is 28.52° N, 103.12° E. (**e**) The geographical location is 27.05° N, 103.35° E. (**f**) The geographical location is 28.45° N, 103.97° E.

Landslide abundance (or landslide density) is commonly used as an index to measure the patterns and characteristics of landslides [15–17]. In this study, landslide number density (LND) was employed to analyze the relationship between influencing factors and landslide occurrence [16,18]. LND is defined as the number of landslides per square kilometer (number/km^2) and is calculated by Formula 1. A low LND value indicates a low likelihood of landslides occurring in the area, while a higher value suggests a greater propensity for landslides.

$$\text{LND} = \frac{\text{The number of landslides in a category}}{\text{Total area in a category}} \quad (1)$$

3.2. Data

Various controlling factors influence the spatial distribution of landslides. Based on previous studies [7,9,10], this study selected six influential factors for analyzing the relationship between different factors and landslides. In this study, ALOS PALSAR DEM

with a 12.5m resolution was selected as the elevation data (https://vertex.daac.asf.alaska.edu/vertex.daac.asf.alaska.edu, accessed on 7 September 2023). Based on the ArcGIS platform, topographic index information was extracted from these DEM data, including slope angle and slope orientation information, which were obtained by ArcGIS software (Figure 3b,d). Information about the river systems was also derived from these DEM data (Figure 3d). Geological unit information was sourced from a 1:200,000 scale geological map published by the China Geological Survey (Figure 1). Rainfall information was sourced from the Loess Plateau Scientific Data Center (http://loess.geodata.cn/, accessed on 11 October 2023) and generated using the Delta spatial downscaling scheme with the global 0.5° climate data released by the Climatic Research Unit (CRU) and the global high-resolution climate data released by Worldclim. By spatially overlaying the average values of each pixel in multiple monthly average precipitation grid images from 2018 to 2022, scale-up was achieved to obtain the 5-year average precipitation data (Figure 3e).

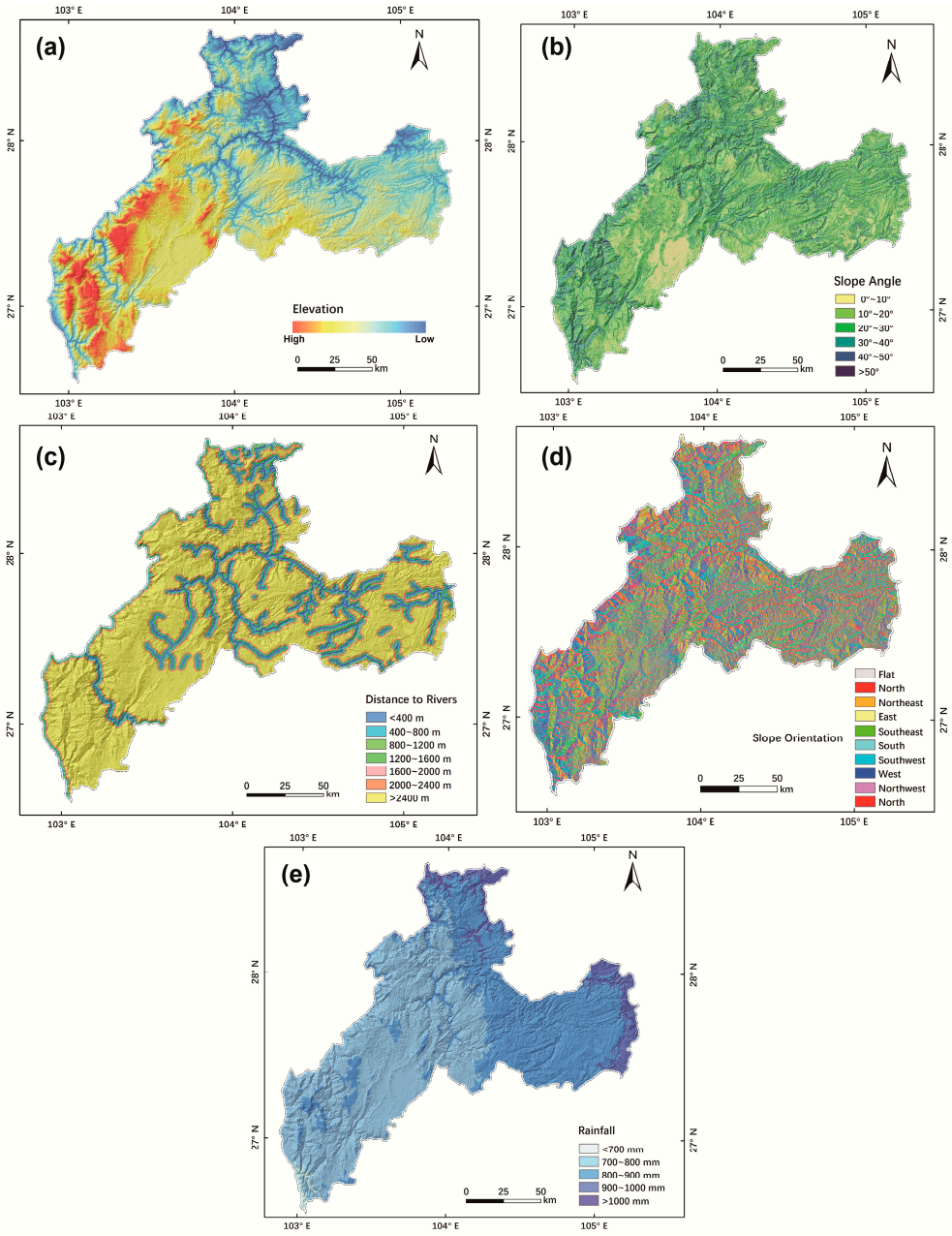

Figure 3. Maps show the distribution of the influencing factors in the study area. (**a**) Elevation; (**b**) slope angle; (**c**) distance to rivers; (**d**) slope orientation; (**e**) rainfall.

Based on the 12.5 m resolution ALOS DEM data, the elevation of the study area was categorized into 14 classes at 200 m intervals: <460 m; 460−660 m; 660−860 m; 860−1060 m; 1060−1260 m; 1260−1460 m; 1460−1660 m; 1660−1860 m; 1860−2060 m; 2060−2260 m; 2260−2460 m; 2460−2660 m; 2660−2860 m; and >2860 m. The slope of the study area ranged from 0° to 83°, and was categorized into six classes at 10° intervals: <10°; 10−20°; 20−30°; 30−40°; 40−50°; and >50°. The slope orientation of the study area was categorized into nine classes: East 67.5−112.5°; South 157.5−202.5°; West 247.5−292.5°; North 337.5−22.5°; Northeast 22.5−67.5°; Southeast 112.5−157.5°; Southwest 202.5−247.5°; Northwest 292.5−337.5°; and flat (−1°). The geological unit of the study area was classified into six types based on the geological era: Quaternary (dominated by sand, mud, clay, and clastic rocks); Neogene (primarily mudstone and clay); Mesozoic (mainly Triassic mudstone and clay); Upper Paleozoic (dominated by Permian basalt); Lower Paleozoic (primarily Ordovician shale); and Pre-Cambrian (dominated by sandstone and clay). Distances to rivers were categorized into seven classes: <400 m; 400−800 m; 800−1200 m; 1200−1600 m; 1600−2000 m; 2000−2400 m; and >2400 m. Rainfall was categorized into five classes at 100 mm intervals: <700 mm; 700−800 mm; 800−900 mm; 900−1000 mm; and >1000 mm.

4. Results

4.1. Landslide Development Characteristics

Through statistical analysis of the distribution of 161 landslides in the Zhaotong area, the results indicate that among the 11 counties in the Zhaotong region, Yiliang County has the highest number of landslide occurrences, with 50 landslides, accounting for 31.06% of all landslides in the area. It is followed by Qiaojia County with 26 landslides, Yanjin County with 19 landslides, and Ludian County with 12 landslides (Figure 4a,c).

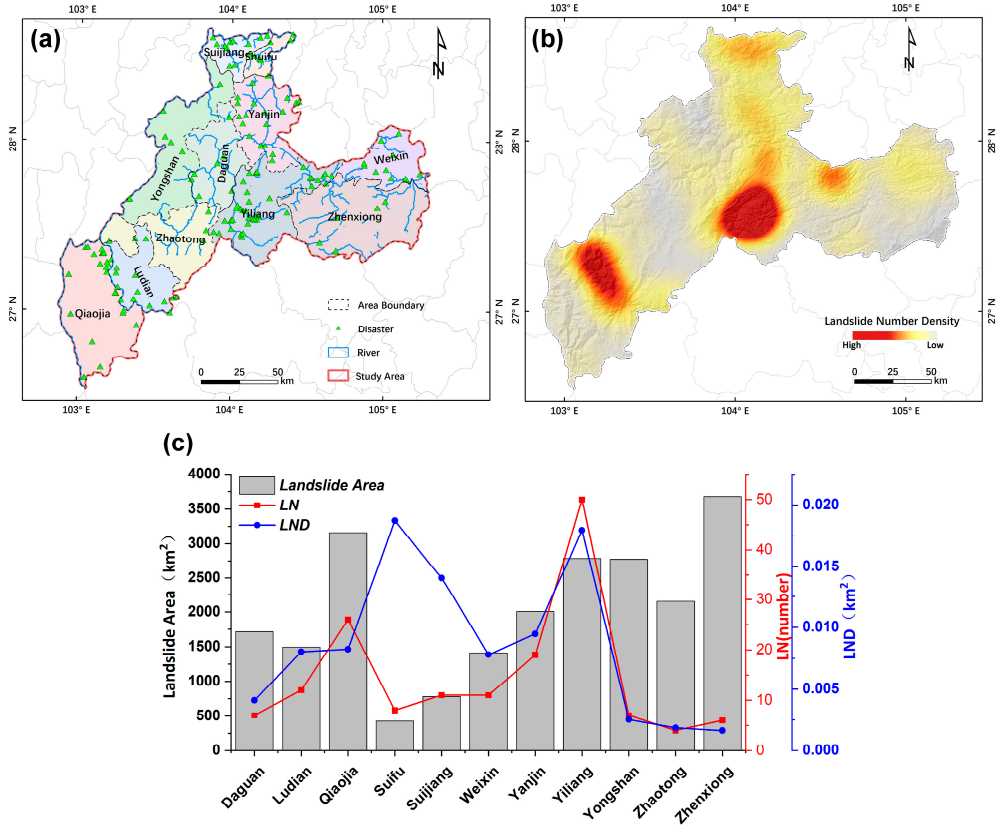

Figure 4. Maps showing the distribution characteristics of landslides. (**a**) Landslide disaster point; (**b**) landslide number density (LND); (**c**) the proportions of LN and LND in each region.

Kernel density analysis refers to calculating the unit density of point data within a specified circular neighborhood, which can effectively analyze the spatial distribution of

point data [19,20]. Based on kernel density analysis of the ArcGIS platform, using landslide information, the LND map can more intuitively reveal the two main areas where landslide number density is concentrated (Figure 4b). The most concentrated occurrences of landslides are observed at the junction of Yiliang County, Zhaotong City, and Daguan County. The second most concentrated area is at the border of Ludian County and Qiaojia County.

4.2. The Relationship between Landslides and Influencing Factors

In areas with significant differences in elevation, due to the large topographical variations, the resistance of soil to gravity decreases, accelerating water flow and increasing soil erosion and dissolution, making landslides more likely to occur [21]. The relationship between landslides and elevation is shown in Figure 5. The elevation range in the study area is from 267 to 4040 m, with an average elevation of 1685 m. The number of landslides within the elevation range of 0 to 1860 m reaches 142, accounting for 88.20% of the total number of landslides. Among them, the number of landslides within the elevation range of 861 to 1060 m is only 25, accounting for 15.53% of the total number of landslides. The number of landslides decreases significantly at elevations greater than 1860 m. Overall, most landslides occur within the elevation range of 0 to 1860 m, with the highest landslide number density occurring within the range of 0 to 660 m. LND gradually decreases with the increase in elevation.

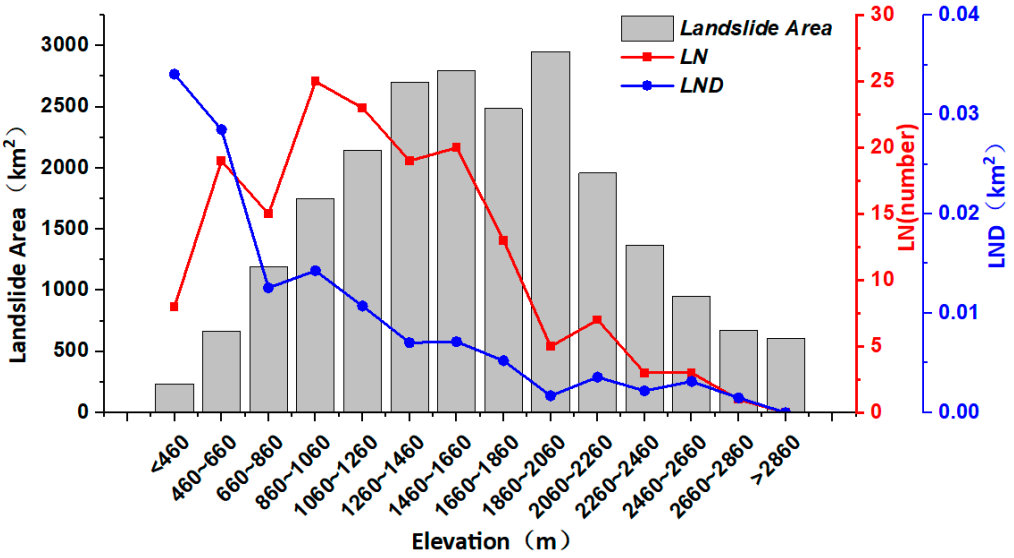

Figure 5. The relationship between landslide distribution and elevation map.

Figure 6 shows the relationship between landslides and slope angle. Slope angle refers to the degree of inclination of the ground and is an indispensable factor leading to landslide occurrences. It generally affects the stability of the slope through the magnitude and direction of the slope body stress, influencing surface runoff and material movement [22]. The results indicate that landslides are concentrated in the ranges of 10° to 30°. The number of landslides within these ranges is 138. The slope range with the highest landslide number density is 30° to 40°, followed by 40° to 50° and 20° to 30°. Overall, the landslide number and LND are relatively low in the slope ranges of <10° and >50°, while they are more triggered in the 10° to 30° range. Figure 7 shows the relationship between landslide distribution and slope orientation, and the statistical result shows that the highest number of landslide occurrences is in the SE direction, with 24, followed by 23 in the N and NW directions. The highest landslide number density occurs in the NE direction, followed by the SE and NW directions. No landslides occurred on flat terrain (−1°).

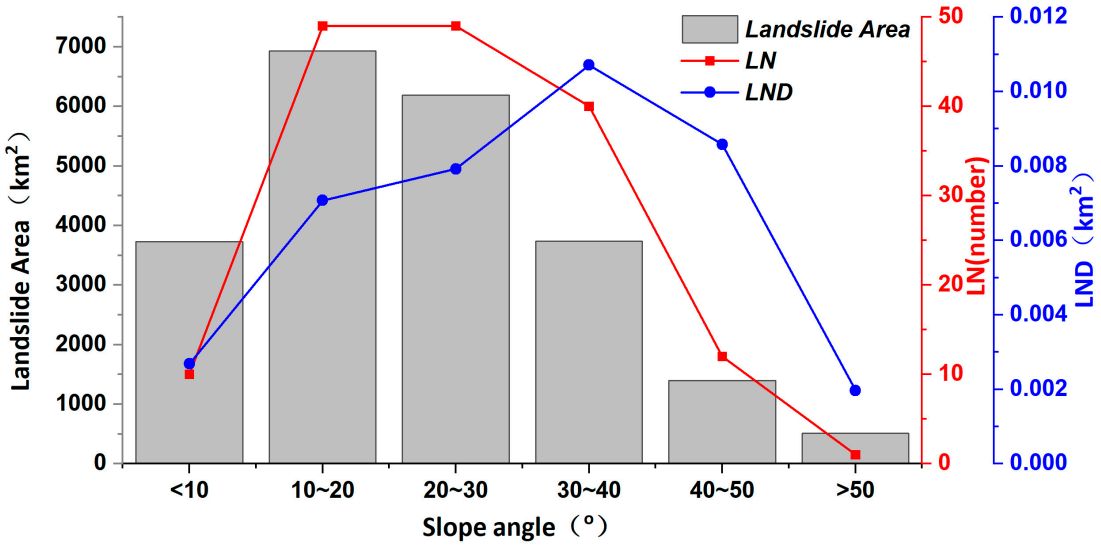

Figure 6. The relationship between landslide distribution and slope angle map.

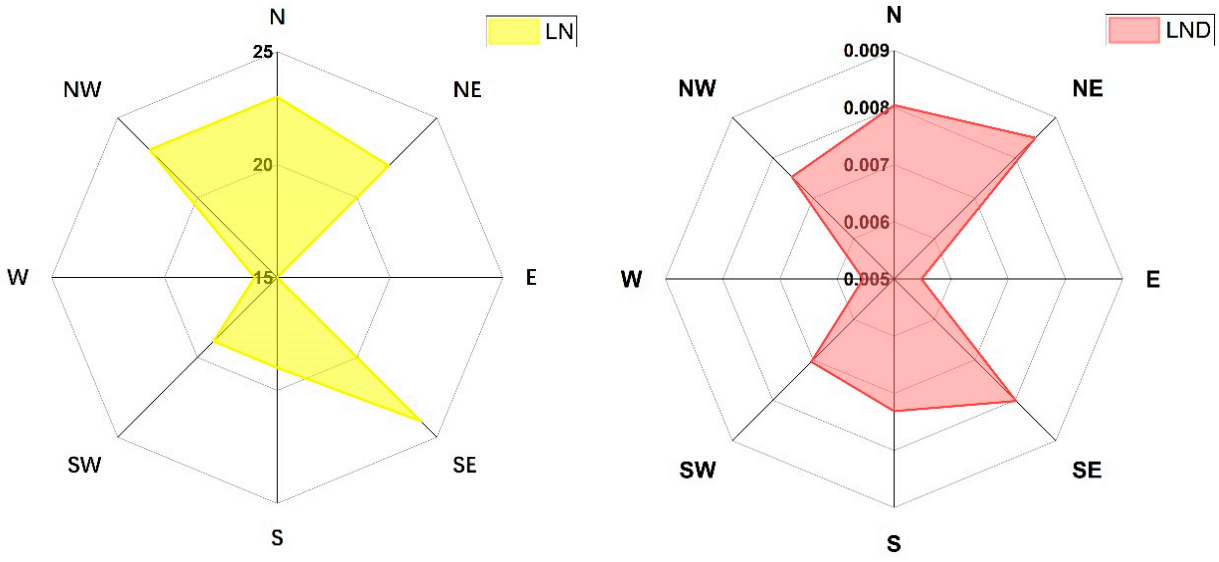

Figure 7. The relationship between landslide distribution and slope orientation map.

The relationship between landslides and geological units is shown in Figure 8, and the results indicate that landslides are mainly concentrated in the Mesozoic, Paleozoic, and Precambrian, with 75, 42, and 41 landslides, respectively. Although the Precambrian, with the highest LND, covers only 210 km^2, landslides mainly occur in the Mesozoic and lower Paleozoic. The Mesozoic is mainly composed of Triassic mudstone and clay, with low mechanical properties of rock and soil mass, and it is sensitive to moisture content, making it prone to landslides. The lower Paleozoic is mainly composed of Ordovician shale, which shows higher mechanical properties of rock and soil mass compared to mudstone and clay, but shale is prone to developing fractures. When rainfall infiltrates, the mechanical properties will decrease, leading to a higher likelihood of landslides. The Paleozoic era, mainly composed of Permian basalt compared to mudstone, clay, and shale, has the highest mechanical properties and lower water permeability, resulting in a low occurrence probability of landslides. There are no landslides occurring in the Quaternary and Neogene.

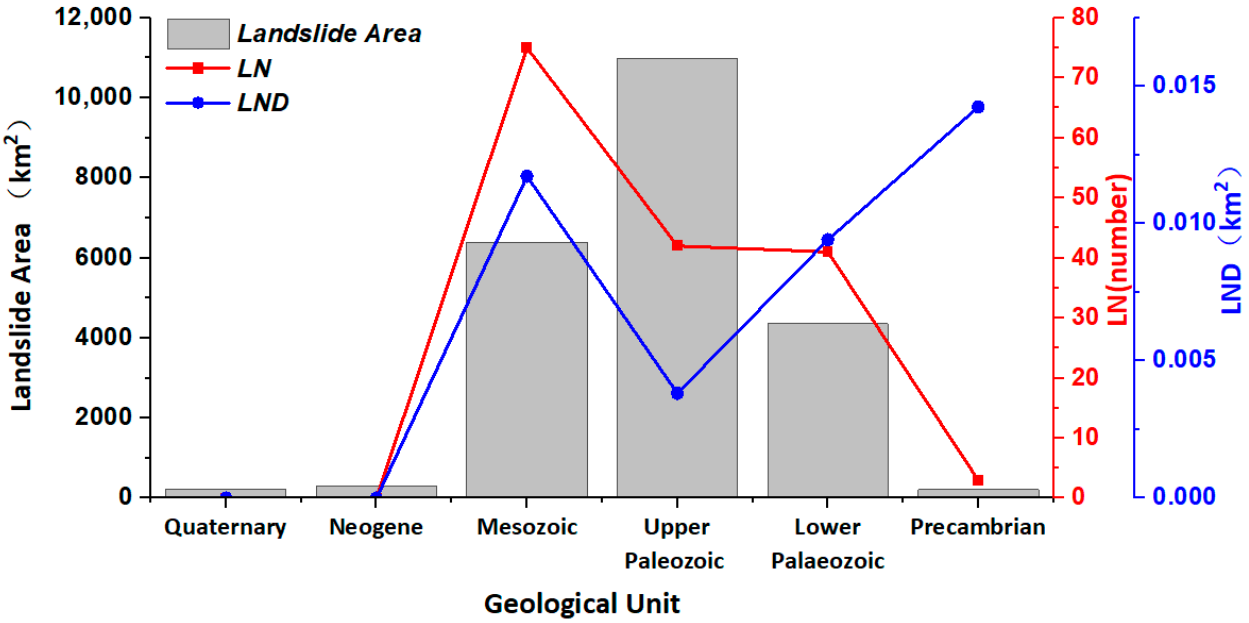

Figure 8. The relationship between landslide distribution and geological unit map.

Rivers also play a role in the development of landslides. When a river flows through a slope, the impact of the water flow can weaken the stability of the slope. Moreover, water from the river infiltrates the soil, increasing the soil's moisture content and saturation, which in turn increases the soil weight, reduces the soil's shear strength, and weakens the slope's stability [23]. The relationship of distance to rivers and landslides indicates that within the range of 0 to 2400 m, both the landslide number and LND decrease with increasing distance from a river. In the <400 m region, the LND is highest, with 48 landslides, accounting for 29.81% of all landslides. Within the range of 2000 to 2400 m, the LND reaches its minimum, with only three landslides, accounting for 1.86% of all landslides. In the >2400 m range, there is a slight increase in LND. Overall, landslides gradually decrease with increasing distance from the river, demonstrating a pronounced negative correlation (Figure 9).

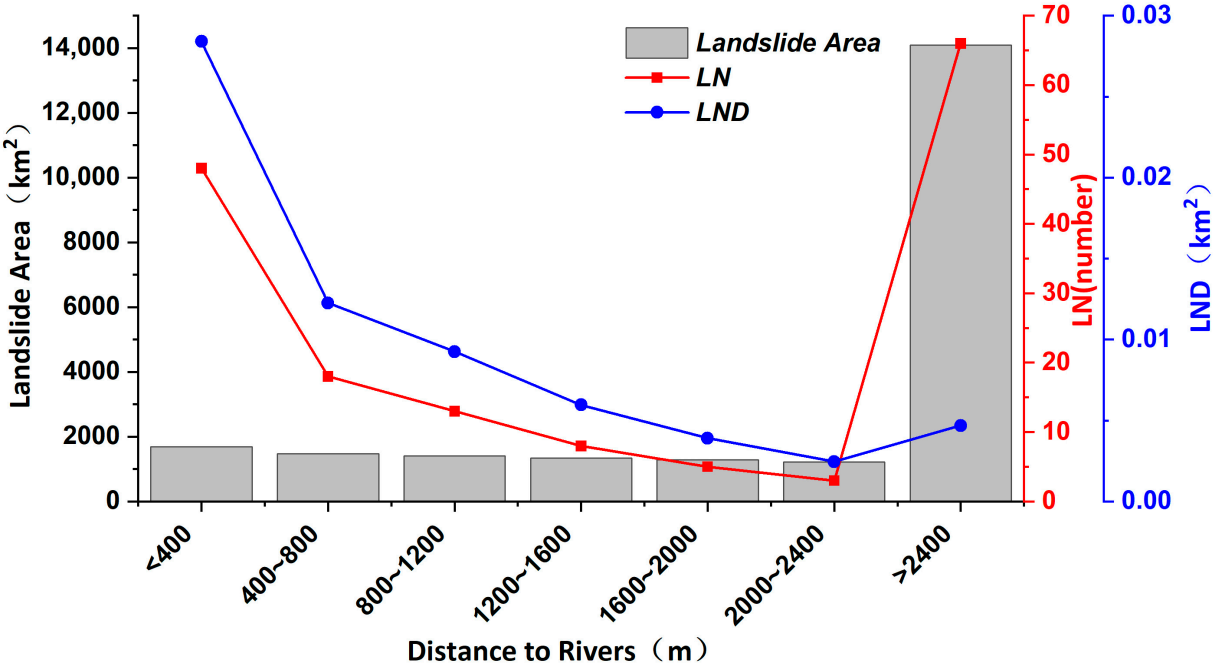

Figure 9. The relationship between landslide distribution and distance to rivers.

The effect of rainfall on landslides is similar to the distance to rivers, i.e., an increase in soil moisture content, leading to an increase in soil pore pressure and a decrease in soil shear strength. When the pore pressure exceeds the soil's shear strength, shear failure occurs and a landslide occurs [24]. The relationship between landslides and rainfall is shown in Figure 10, and the results indicate that the highest number of landslides occur with rainfall ranging from 700 to 800 mm and 800 to 900 mm, at 82 and 54, respectively, accounting for 84.47% of all landslides. The relationship between LND and rainfall shows that LND increases with increasing rainfall, indicating that the greater the rainfall, the higher the likelihood of landslides occurring. When the average rainfall reaches 1000 mm, the maximum LND value reaches 0.04/km^2.

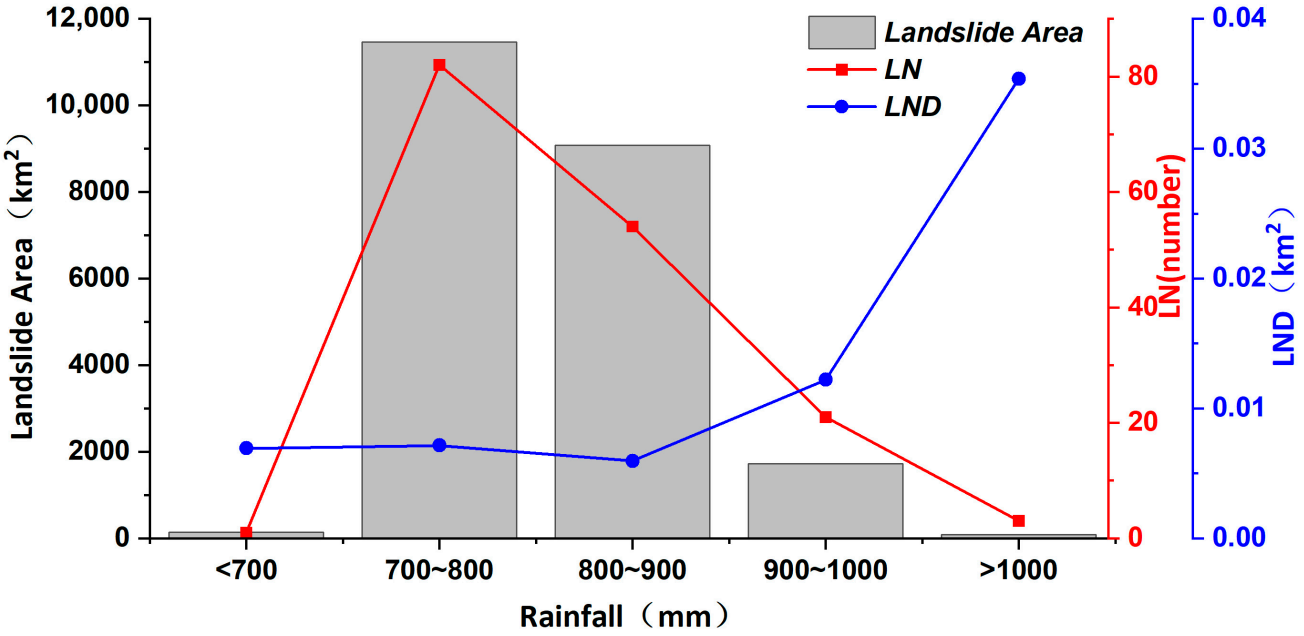

Figure 10. The relationship between landslide distribution and rainfall map.

5. Discussion

Principal Component Analysis (PCA) is an effective multivariate statistical method used to analyze and process the structure of data and variables [25]. It transforms multiple correlated indicators into a few independent composite indicators (principal components) without losing or with minimal loss of the original information. In this study, elevation, slope angle, slope orientation, geological unit, distance to rivers, and rainfall were selected as variables for PCA by SPSS software. The results are presented in Table 1 (Variance Contribution Table) and Table 2 (Loading Coefficient Matrix).

Table 1. Variance Contribution Table of different influencing factors.

Principal Components	Eigenvalue	Variance Contribution Rate %	Cumulative Contribution Rate %
1	2.139	35.648	35.648
2	1.196	19.941	55.589
3	0.947	15.782	771.371
4	0.769	12.814	84.185
5	0.656	10.941	95.126
6	0.292	4.874	100.000

Table 2. Loading Coefficient Matrix of different influencing factors.

Influencing Factors	Principal Component 1	Principal Component 2	Principal Component 3	Principal Component 4
elevation	0.705	0.337	0.233	0.191
slope angle	0.029	0.092	0.978	0.042
slope orientation	0.014	0.041	0.040	0.986
distance to rivers	0.059	0.975	0.104	0.038
rainfall	0.883	0.112	0.087	0.095
geological unit	0.789	0.024	0.046	0.084

Table 1 shows the number of principal components to be extracted. The eigenvalue represents the direction stretching coefficient of each principal component, the variance contribution rate indicates the percentage of original data information reflected after the stretching of the eigenvalue, and the cumulative contribution rate is the sum of these percentages, which is generally greater than 80% in practical applications. According to Table 1, the contribution rate of the first eigenvalue is 35.648%, the second is 19.941%, the third is 15.782%, and the fourth is 12.814%. The cumulative contribution rate of these four eigenvalues is 84.185%, indicating that four principal components should be extracted.

Further analysis of these four principal components reveals their information extraction from the influencing factors, as shown in Table 2, with a loading coefficient standard of 0.4. From Table 2, it can be observed that elevation, rainfall, and geological unit contribute the most to Principal Component 1. Distance to rivers has the highest contribution to Principal Component 2. Slope angle contributes significantly to Principal Component 3, while slope orientation has the largest contribution to Principal Component 4. Thus, it can be concluded that all six influencing factors affect landslides in the Zhaotong area, with elevation, rainfall, and geological unit having the greatest impact. The remaining influencing factors, in order of their contribution, are distance to rivers, slope angle, and slope orientation.

Based on the distance to rivers and elevation, the relationship between landslides and these two influencing factors was further analyzed. As depicted in Figure 11a, a total of 95 landslides were recorded within a distance of 2400 m from the rivers. Within the elevation range of 0 to 1860 m, where the distance to rivers was within 400 m, the highest concentration of landslides was documented, comprising 48 occurrences, representing 50.53% of all landslides within this elevation interval. As the distance from rivers increased, there was a gradual reduction in the number of landslides, accompanied by a corresponding decrease in their proportion. This result shows a possible association between lower elevations and closer proximity to rivers with heightened landslide susceptibility.

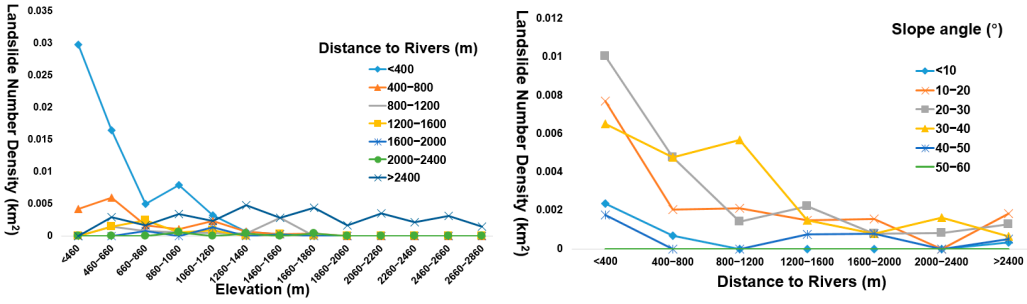

Figure 11. Maps show the relationship between elevation, slope, and distance to river. (**a**) The relationship between elevation and distance to river; (**b**) the relationship between slope angle and distance to river.

Further analysis of the relationship between slope angle and the distance to rivers was conducted. As shown in Figure 11b, for slopes with angles <10° and >40°, there were only

10 landslides, accounting for 10.53% of all landslides within a distance of 2400 m from the rivers; for slope angles ranging from 10° to 40°, most landslides were observed within a distance of 400 m to rivers, at 41, accounting for 43.16% of total numbers. With the increase in the distance to rivers, the number of landslides gradually decreased, and the proportion decreased. Overall, when the slope angle is <10° or >40°, the probability of landslides occurrence is low. For the range with slope angles between 10° and 40° and closer to the river, there is a higher likelihood of landslides occurring. Therefore, effective protective measures should be taken in these areas to prevent the occurrence of landslides.

Moreover, potential geological disasters are widespread in the Zhaotong area, with the vast majority of areas threatened. By analyzing the distribution of 3646 potential geological disasters in the Zhaotong area, it was found that Yiliang County has the highest number of potential geological disasters, with 646, accounting for 17.72% of all potential geological disasters in the area. It is followed by Qiaojia County, Yongshan County, and Daguan County, with the top four counties accounting for more than half of all potential geological disasters. The landslide density map of potential geological disasters was obtained through kernel density analysis as shown in Figure 12a. The most concentrated occurrences of potential geological disasters are observed at Shuifu County, followed by Yiliang County and Daguan County. Comparing the potential geological disaster density (PGDD) with the landslide point density (LND) in Figure 12b, it can be observed that the distribution of potential geological disasters is generally consistent with that of landslides. The areas most threatened are Shuifu County and Yiliang County, while the least threatened areas are Weixin County and Zhenxiong County.

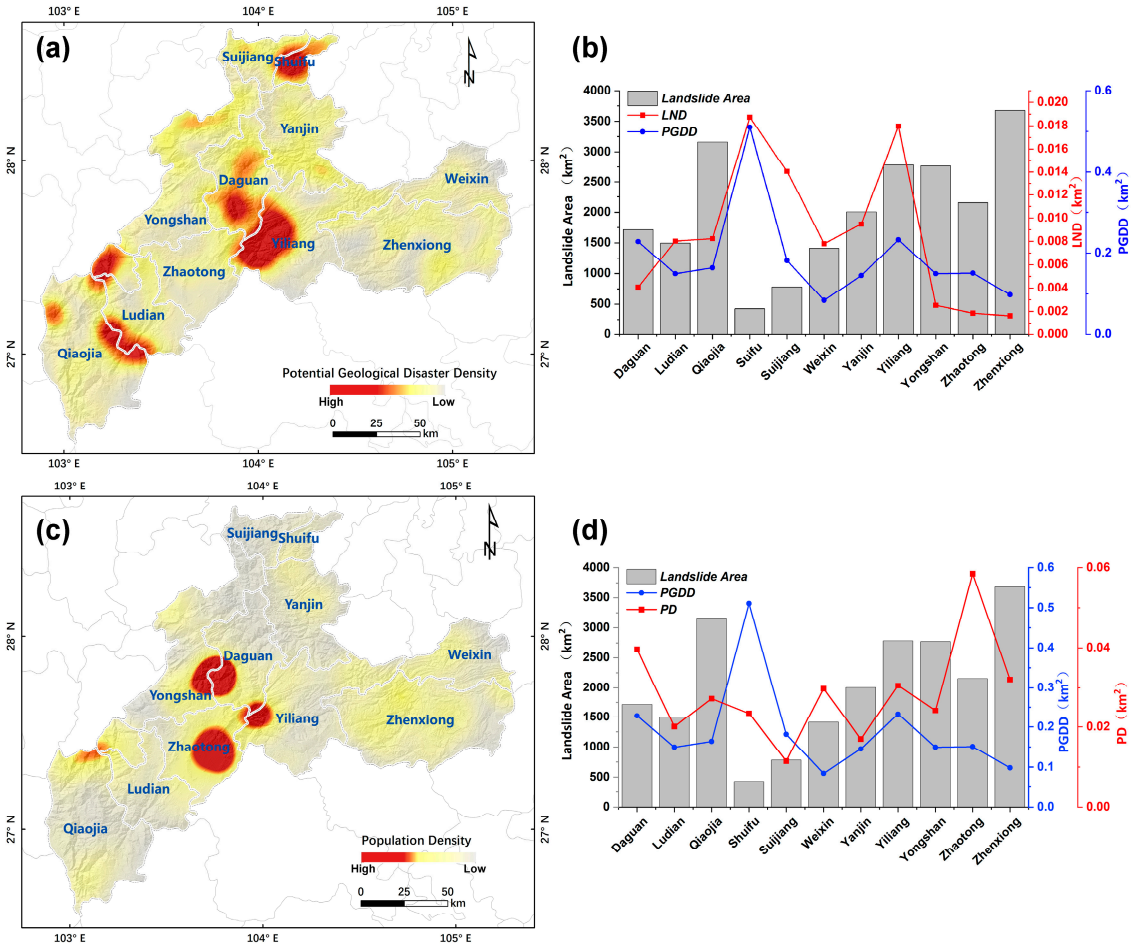

Figure 12. Maps show the relationship between landslide distribution and population distribution. (**a**) Potential geological disaster density (PGDD); (**b**) comparison of PGDD and LND; (**c**) population density (PD); (**d**) comparison of PGDD and PD.

It is essential to analyze the population distribution in the Zhaotong area due to the dense population with a population second only to Kunming City in Yunnan Province. The population density map shows that the most densely populated area is Zhaotong City, followed by Daguan County, Zhenxiong County, Yiliang County, and Weixin County (Figure 12c). By comparing the potential geological disaster density (PGDD) with the population density (PD) in Figure 12d, it can be observed that PD in most areas shows an opposite trend to PGDD. However, Yiliang County and Daguan County are regions with high landslide threat, and they also have relatively dense populations. Therefore, close attention should be paid to the potential geological disasters in these areas. When abnormal phenomena are detected, timely responses can be made to mitigate casualties and property losses.

6. Conclusions

Based on the landslide data provided by the Zhaotong City Natural Resources and Planning Bureau, this study identified 161 landslides and 3646 potential geological disasters based on visual interpretation and the Google Earth platform. Six common influencing factors were selected for spatial distribution analysis of the geohazards of the Zhaotong area. The following conclusions were obtained:

The distribution of potential geological disasters corresponds closely to that of landslides, with the most concentrated landslide occurrences observed at the junction of Yiliang County, Zhaotong City, and Daguan County. The greatest population distribution in the Zhaotong area is opposite to the potential geological disaster density, except for Yiliang County and Daguan County, where the population is relatively dense and landslides are concentrated, which should be paid more attention in terms of regional geological disaster prevention and reduction.

Based on Principal Component Analysis, all six selected influencing factors affect landslide occurrences. Elevation, rainfall, and geological unit have the highest contribution rates, followed by distance to rivers, slope angle, and slope aspect. Landslides primarily occur in the Mesozoic and Lower Paleozoic, with a northeast slope orientation and rainfall ranging from 900 to 1046 mm. Further analysis of the relationship between elevation, slope angle, and distance to rivers indicates that landslides are more likely to occur in the areas with lower elevation and closer proximity to rivers, emphasizing the need for effective protective measures in these areas.

Author Contributions: Writing—original draft, W.W.; Writing—review & editing, S.M.; Supervision, W.Y.; Project administration, R.Y. All authors have read and agreed to the published version of the manuscript.

Funding: This study was supported by the National Natural Science Foundation of China (42307268). We thank Google Earth platform for the free access satellite images used in this study.

Data Availability Statement: The landslides and potential geological disasters inventory of the Zhaotong area are available from the corresponding author upon request. Contact address: yuanrenmao@ies.ac.cn; wwt@ies.ac.cn.

Conflicts of Interest: The authors declare no conflict of interest.

References

1. Xing, A.; Wang, G.; Yin, Y.; Tang, C.; Xu, Z.; Li, W. Investigation and dynamic analysis of a catastrophic rock avalanche on September 23, 1991, Zhaotong, China. *Landslides* **2015**, *13*, 1035–1047. [CrossRef]
2. Wen, W.; Lian, L. Discussion on the Magnitude Assessment to Daguan Jilipu Earthquake on 31 July 1917 inYunnan Province. *Northwestern Seismol. J.* **2010**, *32*, 253–257. (In Chinese)
3. Zhou, J.-W.; Lu, P.-Y.; Hao, M.-H. Landslides triggered by the 3 August 2014 Ludian earthquake in China: Geological properties, geomorphologic characteristics and spatial distribution analysis. *Geomat. Nat. Hazards Risk* **2015**, *7*, 1219–1241. [CrossRef]
4. Qi, S.; Wu, F.; Liu, C.; Ding, Y. Engineering geology analysis on stability of slope under earthquake. *Chin. J. Rock Mech. Eng.* **2004**, *23*, 2792–2797. (In Chinese)

5. Huang, R.; LI, W. A study on the development and distribution rules of geohazards triggered by "5. 12"Wenchuan earthquake. *Chin. J. Rock Mech. Eng.* **2008**, *27*, 2585–2592. (In Chinese)
6. Yin, Y. Research on the geo-hazards triggered by Wenchuan earthquake, Sichuan. *J. Eng. Geol.* **2008**, *16*, 433–444.
7. Zou, Y.; Qi, S.; Guo, S.; Zheng, B.; Zhan, Z.; He, N.; Huang, X.; Hou, X.; Liu, H. Factors controlling the spatial distribution of coseismic landslides triggered by the Mw 6.1 Ludian earthquake in China. *Eng. Geol.* **2022**, *296*, 106477. [CrossRef]
8. Chen, X.-L.; Liu, C.-G.; Wang, M.-M.; Zhou, Q. Causes of unusual distribution of coseismic landslides triggered by the Mw 6.1 2014 Ludian, Yunnan, China earthquake. *J. Asian Earth Sci.* **2018**, *159*, 17–23. [CrossRef]
9. He, X.; Xu, C.; Qi, W.; Huang, Y.; Cheng, J.; Xu, X.; Yao, Q.; Lu, Y.; Dai, B. Landslides Triggered by the 2020 Qiaojia Mw5.1 Earthquake, Yunnan, China: Distribution, Influence Factors and Tectonic Significance. *J. Earth Sci.* **2021**, *32*, 1056–1068. [CrossRef]
10. Jin, J.-L.; Cui, Y.-L.; Xu, C.; Zheng, J.; Miao, H.-B. Application of logistic regression model for hazard assessment of landslides caused by the 2012 Yiliang Ms 5.7 earthquake in Yunnan Province, China. *J. Mt. Sci.* **2023**, *20*, 657–669. [CrossRef]
11. Jia, H.-C.; Chen, F.; Fan, Y.-D.; Pan, D.-H. Comparison of two large earthquakes in China: The Ms 6.6 Yunnan Jinggu Earthquake and the Ms 6.5 Yunnan Ludian Earthquake in 2014. *Int. J. Disaster Risk Reduct.* **2016**, *16*, 99–107. [CrossRef]
12. Sato, H.P.; Harp, E.L. Interpretation of earthquake-induced landslides triggered by the 12 May 2008, M7.9 Wenchuan earthquake in the Beichuan area, Sichuan Province, China using satellite imagery and Google Earth. *Landslides* **2009**, *6*, 153–159. [CrossRef]
13. Xu, C.; Shyu, J.B.H.; Xu, X.W. Landslides triggered by the 12 January 2010 Mw 7.0 Port-au-Prince, Haiti, earthquake: Visual interpretation, inventory compiling and spatial distribution statistical analysis. *Nat. Hazards Earth Syst. Sci. Discuss* **2014**, *14*, 1789–1818. [CrossRef]
14. Zhang, J.; Gurung, D.R.; Liu, R.; Murthy, M.S.R.; Su, F. Abe Barek landslide and landslide susceptibility assessment in Badakhshan Province, Afghanistan. *Landslides* **2015**, *12*, 597–609. [CrossRef]
15. Gorum, T.; Fan, X.; van Westen, C.J.; Huang, R.Q.; Xu, Q.; Tang, C.; Wang, G. Distribution pattern of earthquake-induced landslides triggered by the 12 May 2008 Wenchuan earthquake. *Geomorphology* **2011**, *133*, 152–167. [CrossRef]
16. Xu, C.; Xu, X.; Shyu, J.B.H. Database and spatial distribution of landslides triggered by the Lushan, China Mw 6.6 earthquake of 20 April 2013. *Geomorphology* **2015**, *248*, 77–92. [CrossRef]
17. Xu, C.; Xu, X. Statistical analysis of landslides caused by the Mw 6.9 Yushu, China, earthquake of April 14, 2010. *Nat. Hazards* **2014**, *72*, 871–893. [CrossRef]
18. Migoń, P.; Jancewicz, K.; Różycka, M.; Duszyński, F.; Kasprzak, M. Large-scale slope remodelling by landslides—Geomorphic diversity and geological controls, Kamienne Mts., Central Europe. *Geomorphology* **2017**, *289*, 134–151. [CrossRef]
19. Görüm, T. Tectonic, topographic and rock-type influences on large landslides at the northern margin of the Anatolian Plateau. *Landslides* **2018**, *16*, 333–346. [CrossRef]
20. Bucci, F.; Santangelo, M.; Cardinali, M.; Fiorucci, F.; Guzzetti, F. Landslide distribution and size in response to Quaternary fault activity: The Peloritani Range, NE Sicily, Italy. *Earth Surf. Process. Landf.* **2016**, *41*, 711–720. [CrossRef]
21. ÇEllek, S. Morphological parameters causing landslides: A case study of elevation. *Bull. Miner. Res. Explor.* **2020**, *162*, 197–224. [CrossRef]
22. Dahale, P.P.; Nalgire, T.; Mehta, A.A.; Hiwase, P.D. Slope Stability Analysis by GeoSlope. *Helix* **2020**, *10*, 71–75. [CrossRef]
23. Pourghasemi, H.R.; Pradhan, B.; Gokceoglu, C. Application of fuzzy logic and analytical hierarchy process (AHP) to landslide susceptibility mapping at Haraz watershed, Iran. *Nat. Hazards* **2012**, *63*, 965–996. [CrossRef]
24. Abu Mansor Maturidi, A.M.; Kasim, N.; Abu Taib, K.; Wan Azahar, W.N.A. Rainfall-Induced Landslide Thresholds Development by Considering Different Rainfall Parameters: A Review. *J. Ecol. Eng.* **2021**, *22*, 85–97. [CrossRef]
25. Xu, Z.; Che, A.; Zhou, H. Seismic landslide susceptibility assessment using principal component analysis and support vector machine. *Sci. Rep.* **2024**, *14*, 3734. [CrossRef]